Study of Photo-catalytic Activity of Synthesized Intrinsic and Extrinsic CdS/ZnS Core-shell Nanostructures

Gursharanpal Kaur & Amanjot Kaur & Karamjit Singh*
Department of Physics, Punjabi University, Patiala – 147002, Punjab (India)

Received: May 18, 2018 Accepted: June 18, 2018

ABSTRACT *CdS/ZnS Core-shell nanostructures (NSs) were synthesized by a sonochemical method under ambient conditions. The crystallographic studies of the synthesized materials has been done by X-ray diffraction (XRD) and it shows that the average crystallite size values of pure and Mn^{2+} doped CdS/ZnS core-shell NSs were ~ 4.12 nm and ~ 6.25 nm, respectively. The morphological studies of synthesized core-shell NSs have been done by Field Emission Scanning Electron Microscope (FESEM) and High Resolution Transmission Electron Microscope (HRTEM). Both microscopies reveal the formation of quasi-spherical CdS/ZnS core-shell nanostructures. The optical properties are analysed by UV-Visible spectroscopy. FTIR studies give the information about chemical bonds and identify the chemical species present in synthesized materials. The photo-catalytic activity of intrinsic and extrinsic CdS/ ZnS core-shell NSs has been studied by using methylene blue (MB) as a test contaminant in aqueous media under UV irradiation. In this article, the photo-catalytic activity dependence on the doping concentration has been studied in detailed.*

Keywords: *CdS/ZnS core-shell NSs, Crystallography, Morphology, Photo-catalytic activity, Sonochemical method*

Introduction

II-VI semiconductor nanostructures have been generated great interest in both fundamental studies and technical applications because of their unique size tuneable, optical and electronic properties. In nanostructures materials, more than 80% atoms are on the surface due to high surface to volume ratio. Therefore, surface defects are more prominent in nanostructured materials. The creation of heterostructures such as core-shell nanostructures is the best option to reduce surface defects. Now a day, core-shell heterostructures have attracted considerable attention because of their performance compared with their single components, and these advantages make them one of the most promising candidates for the exploration of new applications in various fields [1-4]. Core-shell semiconductor nanostructures also termed as quantum dots composed of a core and shell made up of different semiconductor nanostructures [5]. The growth of protective shell on the core of nanostructures has demonstrated to be an effective solution to eliminate the surface defects by reducing the number of dangling bonds on the surface and improve the photo stability by physically separating the core surface from its surrounding medium [6,7]. Core-shell nanostructures are potentially useful in optics, optoelectronics, catalysis, chemical engineering and biology [8]. The optical properties of various semiconductors can be enhanced by coating them with a shell of a second higher band gap semiconductor [9]. Commonly discussed core-shell nanostructures include CdSe/ZnS, CdSe/CdS, CdS/ZnS and ZnO/ZnS, where the first semiconductor denotes the core while the second one is the shell of wider band gap than the first [10-12]. Among the different core-shell nanostructures, CdS/ZnS is an interesting one because of its potential applications. Both Cadmium Sulphide and Zinc Sulphide belong to II-VI group chalcogenide semiconductors and have similar crystalline structures (hexagonal and cubic). CdS and ZnS are direct band gap semiconductors with band gap energy of 2.42 eV and 3.7 eV, respectively [13]. Due to higher band gap energy of ZnS, it has been used as surface passivating shell material for CdS [14]. Several reports have been reported on CdS/ZnS core-shell nanostructures. Petr *et.al* [5] reported on molecular modelling of Cd/ZnS core-shell nanoparticles and their photocatalytic activity using Methylene blue as a test contaminant. Qutub *et.al* [15] reported on synthesized CdS/ZnS core-shell and sandwich nanocomposites for photocatalytic properties.

In the present research work, sonochemical method is used for the synthesis of pure and Mn^{2+} CdS/ZnS core-shell nanostructures. Photo-catalytic activity of intrinsic and extrinsic CdS/ZnS core-shell NSs has been thoroughly studied.

Experimental

Materials and chemicals

The chemicals used were of analytical reagent grade and used without any further purification. The AR grade chemicals: zinc acetate $(CH_3COO)_2Zn.2H_2O$, cadmium acetate $(CH_3COO)_2Cd.2H_2O$, thioacetaamide (TAA) (C_2H_5NS) , sodium hydroxide (NaOH), manganese chloride $(MnCl_2.4H_2O)$, ethanol (C_2H_5OH),

methylene blue dye (C_{16} $H_{18}N_3SCl$) were procured from S D Fine Chem Ltd, Mumbai (India) and Loba Chemie, Mumbai (India).

Synthesis of CdS core nanostructures

Sonochemical method [7] already used for synthesis of CdS/ZnS core-shell nanoparticles. With little modifications was used for the synthesis of intrinsic and extrinsic CdS/ZnS core-shell nanostructures. In a typical synthesis, 50 ml of 0.05 M of cadmium acetate and TAA solutions were prepared separately in two different beakers vigorously. Then, the TAA solution was added to cadmium acetate solution drop by drop under continuous stirring. 1M NaOH was added to the stirred solution to keep the pH value constant at about 12. Finally solution was sonicated for 40 minutes. The yellowish precipitates were centrifuged and washed with distilled water and ethanol several times. The settled nanostructures were collected and dried in a vacuum oven at 80^0C. Then synthesized CdS cores were used to produce CdS/ZnS core-shell nanostructures.

Synthesis of pure and doped CdS/ZnS core-shell nanostructures

For synthesis of pure CdS/ZnS core-shell NSs, 50 ml 0f 0.05 M zinc acetate and TAA solutions were prepared separately in two different beakers vigorously. Then 2 g of synthesized CdS core was added to the Zinc acetate solution under magnetic stirring and then added the TAA solution to above solution by drop wise under magnetic stirring. 1 M NaOH was added to the solution to keep the pH value constant at about 12. Finally, the mixture was sonicated for 40 minutes. The light pale yellow prepared core-shell NSs were centrifuged and washed with distilled water and ethanol several times. Later dried in vacuum oven at 80^0C. The pure core-shell nanostructures were obtained. The same procedure was followed for doped core-shell nanostructures. Only difference was the addition of dopant precursor. The dopant precursor ($MnCl_2$) (0.05M) was added to the zinc precursor solution. Different dopant concentrations 10%, 5%, 1%, 0.2% and 0.1% (at.wt %) were added to the zinc acetate solution to check the dopant concentration dependent photocatalytic behaviour of synthesized core-shell nanostructures.

Characterization

The structural and phase composition of the core-shell nanostructures was analyzed by powder X-ray diffraction. The diffraction patterns were recorded in 2θ range of 20^0 -70^0 using Rigaku Miniflex-600 X-ray powder diffractometer by using Cu K_α radiation (λ = 1.54056). The surface morphology of characterized core-shell NSs was studied by Field Emission Scanning Electron Microscopy (FESEM). FESEM micrographs were recorded at 3.00kV accelerating voltage. High Resolution Transmission Electron Microscope (HRTEM) was used to determined the particle size distribution. For TEM micrographs, CdS/ZnS NSs were well dispersed in DMF and sonicated for 15 minutes and after this placed the drop of this solution on the carbon-coated copper grid and analysed by Hitachi[(H-7650), Japan] Transmission Electron Microscope at accelerating voltage of 100keV. The chemical bonds and chemical species were analysed with Model RZX (Perkin Elmer) Fourier Transform (FTIR) Infra-red Spectrophotometer in the wavenumber range of 4000 cm^{-1} - 400 cm^{-1}. UV-visible absorption spectra were recorded in the wavelength range of 300 nm – 650 nm by using Hitachi (2J-0004) spectrophotometer. For UV-visible absorption spectra, 10mg of core-shell NSs were dispersed in 10 ml of solvent (DMF) and sonicated. When the solute was completely soluble in DMF then measurements were taken in UV-visible spectrophotometer.

Photo-catalytic Activity

The photo-catalytic activity of synthesized intrinsic and extrinsic CdS/ZnS core-shell NSs was studied by the degradation of Methylene Blue (MB) dye as a test contaminant in aqueous media under the UV radiation with continuous magnetic stirring. Methylene Blue (MB) stock solution was prepared by dissolving 0.003 mg dye into 1000 ml of distilled water. Then taken 100 ml of prepared dye solution and add 0.01g of synthesized core-shell nanostructures. Placed the mixture in dark with continuous magnetic stirring for 1 hour, for complete adsorption of dye on the surface of core-shell nanostructures. Then taken a 10 ml sample from suspension in test-tube. The remaining suspension was irradiated in laboratory made UV reactor (two 18-W UV tube, λ =200 to 400 nm) used as UV source. The suspension was irradiated for 80 minutes in UV exposure. After every 10 minutes, 10 ml of suspension was removed out for testing. Repeat the above process till 80 minutes. All collected samples were analysed in UV-visible spectrophotometer to check the degradation of MB dye. Same steps were followed for different doping concentrations of core-shell NSs.

Results and Discussion

Crystallographic analyses

The recorded XRD patterns of pure and 10% Mn doped CdS/ZnS core-shell nanostructures are shown in Fig. 1(a, b). The recorded diffractograms of samples are agreed well with the standard peaks of cubic structure of CdS (JCPDS file no: 42-1411) [16], and with hexagonal structure of ZnS (JCPDS file no: 05-0492[17]. In Fig.1 (a), the observed diffraction peaks of CdS at $2\theta = 44.49^0$ and 52.19^0 are associated with (220) and (311) planes and ZnS at $2\theta = 27.41^0$, 28.76^0, 36.05^0 and 47.89^0 are associated with (100), (002),(102) and (103) planes, respectively. In Fig. 1(b), there is slight shifting in diffractions peaks, this is may be due to Mn^{2+} doping. The diffraction peaks at $2\theta = 27.46^0$, 28.78^0, 33.40^0, 36.19^0, 44.41^0, 47.80^0 and 51.78^0 are observed corresponds to similar crystal planes. The weak diffraction peaks at $2\theta = 42.05^0$, 61.08^0 and 67.8^0 are associated with (110), (206) and (203) planes were also observed in Fig. 1(b). The recorded diffraction peaks have broadening due to the formation of nanocrystallites. The average crystallite size was calculated by using Debye-Scherrer's formula [18] as given below:

$$D = 0.89\lambda/\beta\cos\theta \quad \text{----------} \quad \text{(i)}$$

In equation (i), 0.89 is the constant value for shape factor, λ is the X-ray wavelength of Cu Kα X-ray, β is the full width half maximum(FWHM) of the highest peak and θ is the Bragg diffraction angle. The calculated average crystallite sizes are ~ 2.67 nm and 4.11 nm for pure and doped CdS/ZnS core-shell nanostructures respectively. There is increase in size of core-shell with Mn^{2+} doping. This may be due to the large ionic radii of Mn^{2+} (88 pm) as compared to Zn^{2+} (81 pm).

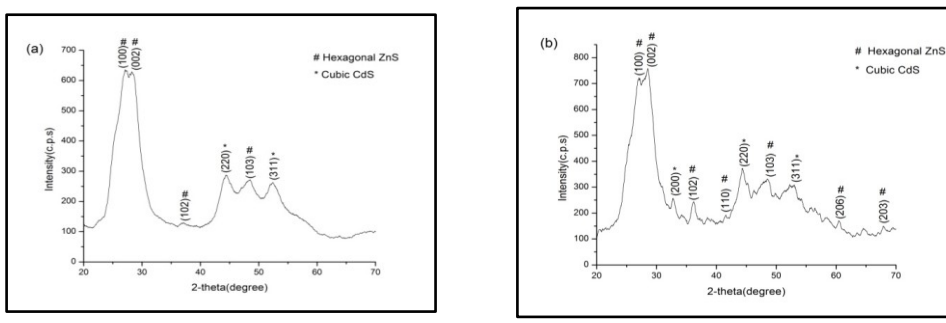

Fig. 1 XRD Pattern of (a) Pure CdS/ZnS core-shell NSs (b) 10% Mn doped CdS/ZnS core-shell NSs

Morphological studies

Fig. 2 (a, b) displays the FESEM images of pure and 10% Mn doped CdS/ZnS core-shell nanostructures. Both images show that core-shell nanostructures are spherical and quasi-spherical in shape. Moreover, recorded micrographs show that the size of CdS/ZnS core-shell NSs is increased with Mn doping.

Fig. 3 (a, b) shows the recorded TEM micrographs of pure and 10% Mn doped CdS/ZnS core-shell NSs, respectively. It can be clearly seen from TEM micrographs that core-shell NSs are formed with slight agglomeration. The average particle size calculated from TEM micrographs are ~ 20.5 nm and ~ 23.9 nm for pure and 10% Mn doped CdS/ZnS core-shell NSs, respectively. There is small change in average particle size with Mn doping in CdS/ZnS core-shell NSs.

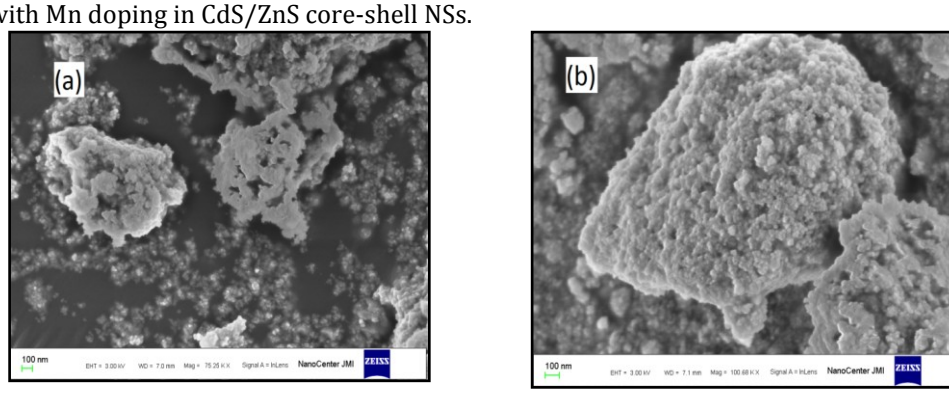

Fig. 2 FESEM micrographs of (a) Pure CdS/ZnS core-shell NSs (b) 10% Mn doped CdS/ZnS core-shell NSs

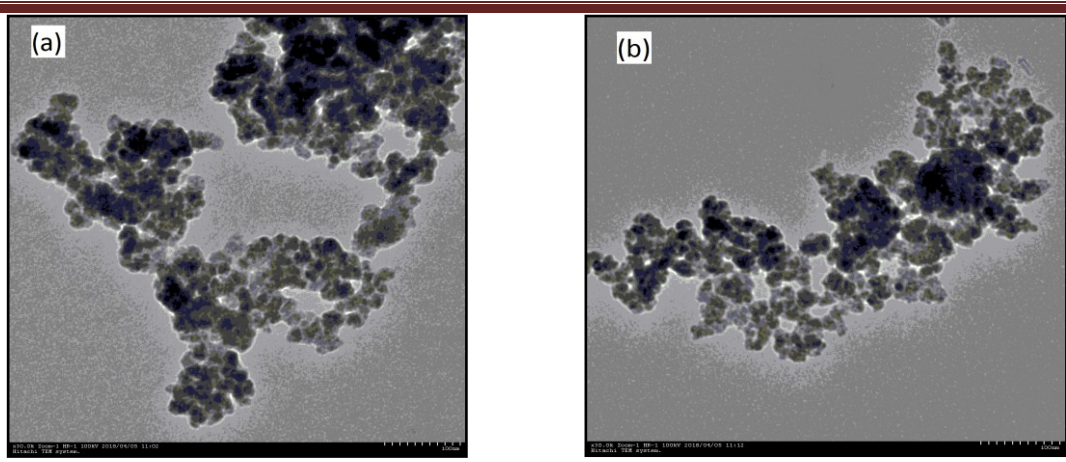

Fig. 3 TEM Micrographs of (a) Pure CdS/ZnS core-shell NSs (b) 10% Mn doping CdS/ZnS core-shell NSs

Fourier Transform Infrared (FTIR) analyses

Fig. 4 (a, b) shows the recorded FTIR spectra of pure and 10% Mn doped CdS/ZnS core-shell nanostructures in the range of 4000 – 400 cm^{-1}. In FTIR, by comparing the recorded spectra with standard database, it is observed that peaks at 3433.1cm^{-1} and 16.29cm^{-1} are due to stretching vibration of O-H bond of H_2O molecule [19]. The presence of characteristic peaks at 2127.7cm^{-1}, 1462.2cm^{-1}, (1414.3cm^{-1}, 1010.4cm^{-1}) and 1169.5cm^{-1} due to C≡C triple bond, C-O stretching, CH_2 bending and C-O-C out of phase stretching[20,21]. A peak observed at 932.0cm^{-1} is due to Zn-S vibrations [22]. The peaks observed between 400-700 cm^{-1} indicates the formation of Zn-S and Cd-S bonds and this region is assigned to Metal-Sulphur bond [20, 23]. In doped core-shell NSs, the peaks are slightly shifted due to the presence of additional metal bonds caused by doping in ZnS shell.

Table 1: The description of functional groups present in pure and 10% Mn doped CdS/ZnS core-shell NSs

Functional groups	Pure CdS/ZnS core-shell NS stretching frequencies(cm^{-1})	10% Mn doped CdS/ZnS core-shell NS stretching frequencies(cm^{-1})
O-H stretching	3433.1, 1629.3	3448.0, 1630.4
C≡C triple bond	2127.7	2139.7
C-O stretching	1462.2, 1010.4	1466.1, 1013.3
CH_2 bending	1414.3	---
C-O-C stretching	1169.5	1173.7
Zn-S vibrations	932.0	---
Zn-S & Cd-S stretching vibrations	659.8, 608.2,473.1	654.7, 534.1

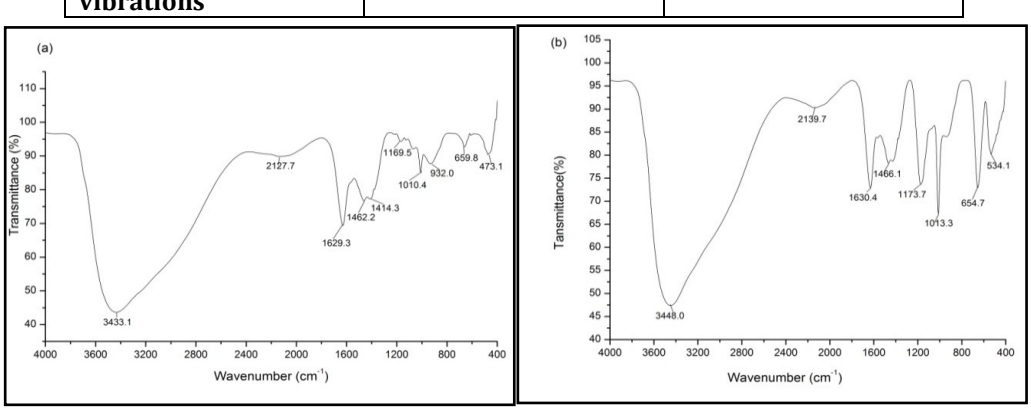

Fig. 4 FTIR spectra of (a) Pure CdS/ZnS core-shell NSs (b) 10% Mn doped CdS/ZnS core-shell NSs

UV-Visible spectroscopic studies analyses

Fig. 5 shows the UV-Visible absorption spectra of pure and 10% Mn doped CdS/ZnS core-shell NSs. The recorded spectrum has broad absorption profiles in the UV-Visible range of electromagnetic spectrum and this makes core-shell nanostructures suitable for photo-catalytic activity. Fig. 5 shows that the absorbance of 10% Mn doped CdS/ZnS core-shell is less than pure CdS/ZnS core-shell nanostructure in the UV-Visible region. So it seem that pure CdS/ZnS core-shell NSs may show better photo-catalytic activity as compared to 10% Mn doped CdS/ZnS core-shell NSs in UV-Visible region.

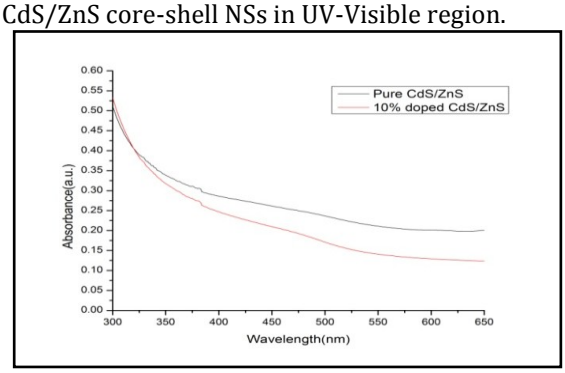

Fig.5 UV-Vis Absorption spectra of (a) pure CdS/ZnS core-shell NSs (b) 10% Mn doped CdS/ZnS core-shell NSs

Photo-catalytic Activity analyses

The photo-catalytic degradation of MB dye as test contaminant in aqueous media was investigated using synthesized pure CdS/ZnS and Mn doped (Doping concentration: 10%, 5%, 2%, 1%, and 0.1% at.wt %) CdS/ZnS core-shell NSs under UV irradiation. The absorption spectra of MB dye solution for different durations of UV- Visible irradiation for different concentrations are plotted between wavelength and absorbance as shown in Fig. 6 (a –f). According to Beer-Lambert's law, the concentration of MB dye is linearly proportional to the intensity of the absorption peak at 663nm and thus the decoloration of MB dye can be calculated using the following expression:

$$\textbf{Degradation Rate (\%)} = (1-A_t/A_0)\times 100 \qquad \text{------ (ii)}$$

In equation (ii), A_t and A_0 are absorption of dye at't' time and at initial time respectively. Fig. 7 shows the degradation profile of MB dye solution for different durations of UV-Visible irradiation. For photo-catalytic activity, the stock solution with core-shell NSs was stirred for one hour in the dark, so as to adsorb dye on its surface. After one hour , at 0min the dye concentration in a case of pure CdS/ZnS, 0.1%, 1%, 2%, 5% and 10% Mn doped CdS/ZnS core-shell NSs is 90.5%, 74.6%, 85.9%, 76.1%, 78% and 53.9%, respectively. It is clear from Fig.7 the adsorption of dye in dark is more in a case of 10% Mn doped CdS/ZnS core-shell NSs whereas the adsorption of dye in dark is less in a case of pure CdS/ZnS core-shell NSs. The reason is that with doping the size of core-shell NSs is increased and hence the surface area increased. So 10% Mn doped CdS/ZnS core-shell NSs have adsorbed more dye on its surface as compared to pure CdS/ZnS core-shell NSs. It is also clearly seen from Fig. 7, the photo-catalytic degradation of MB dye in UV irradiation for pure CdS/ZnS core-shell NSs is maximum as compared to different concentrations of Mn doping in CdS/ZnS core-shell NSs. The MB dye is degraded to maximum (42.6%) extent in a case of pure CdS/ZnS core-shell NSs whereas it is degraded to minimum (45.3%) in a case of 10% Mn doped CdS/ZnS core-shell NSs at 80mins of UV irradiation. The enhanced photo-catalytic activity of pure CdS/ZnS core-shell NSs can be explained by the photo-generated electron (e^-) and hole (h^+) pairs. When the UV photon interacts with CdS/ZnS core-shell NSs dispersed in MB dye contaminated aqueous solution, the photo-excited carriers (e^- and h^+) are generated. There are two major possibilities either photo-excited e^- and h^+ can recombine through radiative emission process or these can be trapped in defect states followed by recombination or else transferred to the core-shell NSs surface, where these may counter with species adsorbed on or close to the surface of the particles [17]. In a case of pure CdS/ZnS core-shell NSs, based on their energy band levels all the photo-generated electrons and holes are moved to the conduction band (CB) and valence band (VB) of CdS. In the oxygen equilibrated media, the photo-excited electrons are scavenged by molecular oxygen O_2 to hydrogen peroxide H_2O_2 and the superoxide radical anion O_2^-, these intermediates radicals interact to generate hydroxyl radicals •OH and these radicals degrade the dye molecule [9]. However the hole formed in the VB of CdS cannot produce oxidize hydroxyl radicals and H_2O molecule. But furthermore, it can oxidize organic dye molecules into reactive intermediates and final products. In addition, in the CdS/ZnS core-shell NSs, both the energy levels are displaced symmetrically into

the core material (CdS) because of the shell material (ZnS) has a larger band gap. Furthermore, the outer electron and hole are relaxes in to the core material when the shell nanoparticles are excited. The following reasons are responsible for enhanced photocatalytic activities of CdS/ZnS core-shell NSs (i) the shell material effectively passivate the surface electron states of the CdS core level. (ii) The surface charge modification, inhibition of CdS photo-corrosion and surface electronic state passivation of CdS core material [23]. But in a case of 10% Mn doped CdS/ZnS core-shell NSs, Mn^{2+} ions are trapped into the deep energy levels of CdS/ZnS core-shell NSs. The photo-generated e^- and h^+ are recombined due to trapping at deep Mn^{2+} defect states caused in Mn^{2+} doped CdS/ZnS core-shell NSs. So there are lesser number of charge carriers present at the surface of Mn^{2+} doped CdS/ZnS core-shell NSs to participate in photo-catalytic degradation of MB dye. Hence with Mn doping in CdS/ZnS core-shell NSs, the photo-catalytic activity of CdS/ZnS core-shell NSs is decreased.

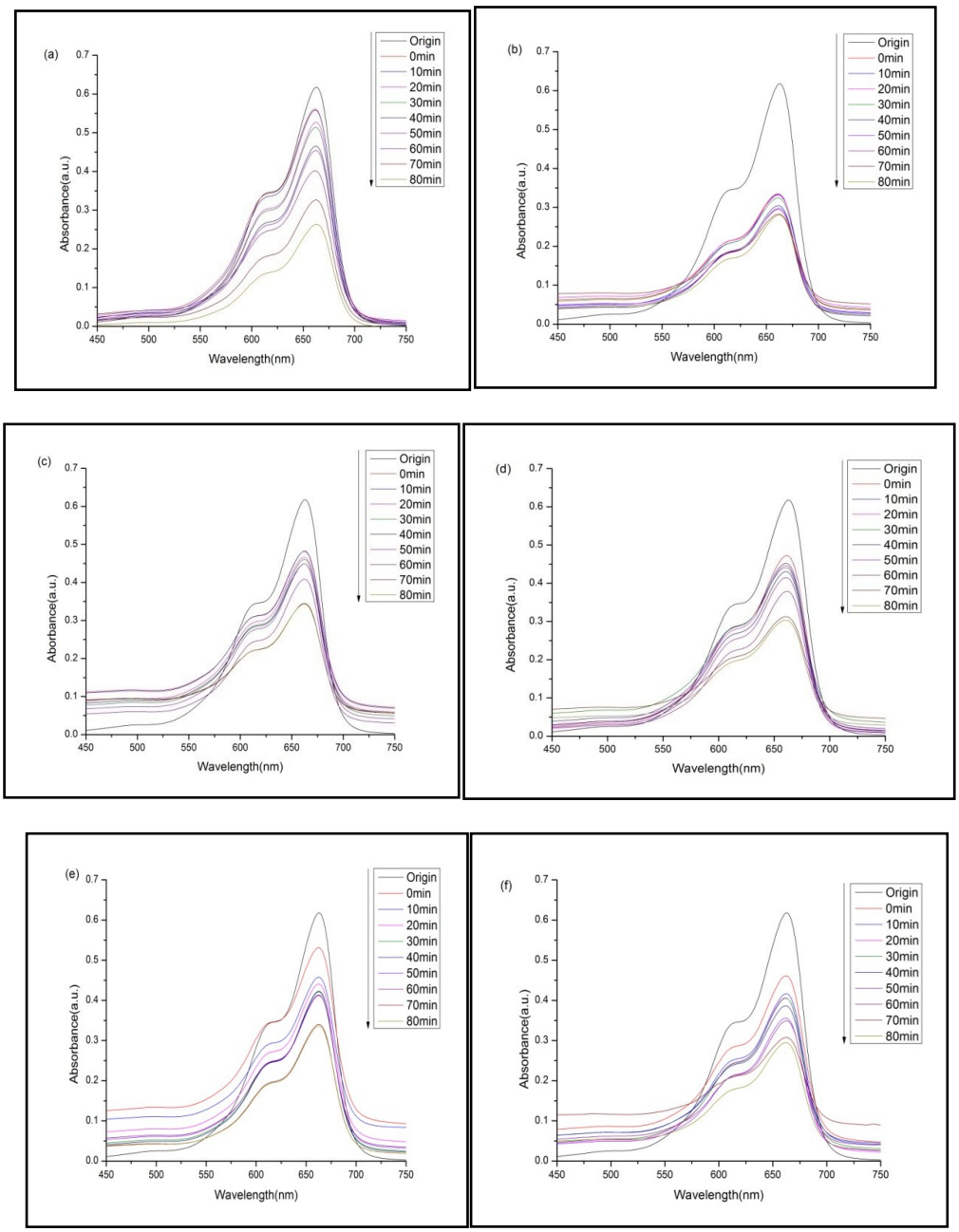

Fig.6 Photo-catalytic degradation of MB dye by (a) Pure CdS/ZnS core-shell NSs (b) 10% Mn doped CdS/ZnS core-shell NSs (c) 5% Mn doped CdS/ZnS core-shell NSs (d) 2% Mn doped CdS/ZnS core-shell NSs (e) 1% Mn doped CdS/ZnS core-shell NSs (f) 0.1% Mn doped CdS/ZnS core-shell NSs

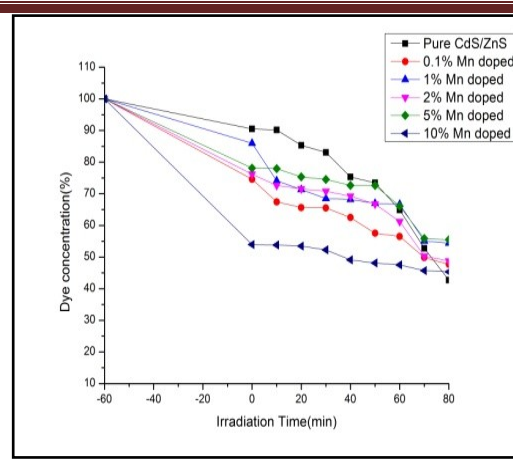

Fig.7 Degradation Profile of MB dye with UV irradiation time in the presence of intrinsic and extrinsic CdS/ZnS core-shell NSs

Conclusions

Pure and Mn doped CdS/ZnS core-shell NSs are successfully synthesized by sonochemical method. XRD results confirms the formation of CdS/ZnS core-shell NSs with the hexagonal phase of ZnS and cubic phase of CdS having average crystalline size values ~ 2.67 nm and 4.11 nm for pure and Mn doped CdS/ZnS core-shell NSs, respectively. FESEM and TEM results show the formation of spherical and quasi-spherical agglomerated core-shell NSs having average particle size values ~ 20.5 nm and ~ 23.9 nm for pure and 10% Mn doped CdS/ZnS core-shell NSs, respectively. FTIR spectra confirm the formation of pure and 10% Mn doped CdS/ZnS core-shell NSs by bending and stretching modes of CdS and ZnS NSs. The UV-Visible absorption spectra show that the synthesized core-shell NSs can be photo-excited in the UV-Visible range of electromagnetic spectra for photo-catalytic applications. The photo-catalytic activity potential of the synthesized core-shell NS under UV irradiation tested using MB dye as a test contaminant in aqueous media reveal that the synthesized NSs are efficient photocatalysts. Due to higher surface to volume ratio and interface actions, pure CdS/ZnS core-shell NSs exhibited higher photo-catalytic activity as compared to Mn doped CdS/ZnS core-shell NSs. Due to low surface to volume ratio, dopant concentration deteriorates photo-catalytic activity of CdS/ZnS core-shell NSs via the recombination of trapped carriers. These synthesized core-shell NSs with augmented photo-catalytic activity can be efficiently used for purification of the polluted water.

Acknowledgment

The authors are highly thankful for instrumentation facility provided by Sophisticated Instruments Centre, Punjabi University Patiala. The authors are also grateful to SAIF, Panjab University, Chandigarh for FTIR analyses and PAU, Ludhiana for HRTEM analyses. The authors are highly thankful to Centre of Nanoscience and Nanotechnology, Jamia Millia Islami University, New Delhi for FESEM analyses.

References

[1] S. Wei, Q. Wang, J. Zhu, L. Sun, H. Lin, Z. Guo, Multifunctional Composite Core-shell Nanoparticles, Nanoscale 3 (2011) 4474–4502.
[2] R.G. Chaudhuri, S. Paria, Core/shell Nanoparticles: Classes, Properties, Synthesis Mechanisms, Characterization and Applications, Chem. Rev. 112 (2012) 2373–2433.
[3] H. Wang, L. Chen, Y. Feng, H. Chen, Exploiting Core-shell Synergy for Nanosynthesis and Mechanistic Investigation, Acc. Chem. Res. 46 (2013) 1636–1646.
[4] P. Hu, J. V. Morabito, C. K. Tsung, Core-shell Catalysts of Metal Nanoparticle Core and Metal-organic Framework Shell, ACS Catal. 4 (2014) 4409–4419.
[5] P. Praus, L. Svoboda, J. Tokarsy, A. Hospodkova, V. Klemm, Core/shell CdS/ZnS Nanoparticles: Molecular Modelling and Characterization by Photocatalytic Decomposition of Methylene Blue, Appl. Surf. Sci 292 (2014) 813-822.
[6] L. Huang, X. Wang, J. Yang, G. Liu, J. Han, C. Li, Dual Cocatalysts Loaded Type I CdS/ZnS Core/shell Nanocrystals as Effective and Stable Photocatalysts for H_2 evolution, J. Phys. Chem. C 117 (2013) 11584-11591.
[7] O. Amiri, S. M. H. Mashkani, M. M. Rad, F. Abdvali, Sonochemical Synthesis and Characterization of CdS/ZnS Core–shell Nanoparticles and Application in Removal of Heavy Metals from Aqueous Solution, Superlattices Microstruct. 66 (2014) 67–75.

[8] F. Caruso, Nanoengineering of Particle Surfaces, Adv. Mater. 13 (2001) 11.
[9] N. Qutub, B. M. Pirzada, K. Umar, O. Mehraj, M. Muneer, S. Sabir, Synthesis, Characterization and Visible-Light Driven Photo Catalysis by Differently Structured CdS/ZnS Sandwich and Core–shell Nano Composites, Physica E 74 (2015) 74–86.
[10] M. A. Malik, P. O'Brien, N. Revaprasadu, A Simple Route to the Synthesis of Core/Shell Nanoparticles of Chalcogenides, Chem. Mater. 14 (2002) 2004-2010.
[11] J. Liu, C. Zhao, Z. Li, J. Chen, H. Zhou, S. Gu, Y. Zeng, Y. Li, Y. Huang, Low-temperature Solid-state Synthesis and Optical Properties of CdS–ZnS and ZnS–CdS Alloy Nanoparticles, J. Alloys Compd. 509 (2011) 9428-9433.
[12] F. Li, Y. Jiang, L. Hu, L. Liu, Z. Li, X. Huang, Structural and Luminescent Properties of ZnO Nanorods and ZnO/ZnS Nanocomposites, J. Alloys Compd. 474 (2009) 531-535.
[13] C. W. Raubach, Y. V. B. Santana, M. M. Ferrer, V. M. Longo, J. A. Varela, W. A. Jr., P. G. C. Buzolin, J. R. Sambrano, E. Longo, Structural and Optical Approach of CdS@ZnS Core-shell System, Chem. Phys. Lett. 536 (2012) 96-99.
[14] X. F. Duan, C. M. Niu, V. Sahi, J. Chen, J. W. Parce, S. Empedocles, J.L. Goldman, High-performance Thin-film Transistors using Semiconductor Nanowires and Nanoribbons, Nature 425 (2003) 274-278
[15] A. R. B. Suganthi, P. Sagayaraj, Modified Solvothermal Synthesis and Characterization of CdS/ZnS Core/shell Nanorods, Mater. Chem. Phys. 139 (2013) 917–922.
[16] C. V. Reddy, J. Shim, M. Cho, Synthesis, Structural, Optical and Photocatalytic Properties of CdS/ZnS Core/shell Nanoparticles, J. Phys. Chem. Solids 103(2017) 203-217.
[17] B. Kaur, K. Singh, A.K. Malik, Effect of Ligands on Crystallography, Morphology and Photo- catalytic Ability of ZnS Nanostructures, Dyes Pigm. 114(2017)153-160.
[18] M. Chitkara, K. Singh, I. S. Sandhu, H. S. Bhatti, Photo-catalytic Activity of $Zn_{1-x}Mn_xS$ Nanocrystals, Nanoscale Res. Lett. 6 (2011) 438
[19] A. Roychowdhury, S. P. Pati, S. Kumar, D. Das, Effects of Magnetite Nanoparticles on Optical Properties of Zinc Sulfide in Fluorescent-magnetic Fe_3O_4/ZnS Nanocomposites, Powder Technol. 254 (2014) 583-590.
[20] Z. K. Heiba, M. B. Mohamed, N. G. Imam, Hybrid Luminescent CdS@ZnS Nanocomposites, Ceram. Int. 41 (2015)12930-12938.
[21] R. Seoudi, A. B. E. Bailly, W. Eisa, A. A. Shabaka, S. I. Soliman, R. K. A. E. Hamid, R.A. Ramadan, Synthesis, Optical and Dielectric Properties of (PVA/CdS) Nanocomposites, J. Appl. Sci. Res. 8 (2012) 658-667.
[22] N. M. Ravindra, V. K. Srivastava, Variation of Refractive Index with Energy Gap in Semiconductors, Infrared Phys. 19 (1979) 603–604.
[23] S. Ummartyotin, N. Bunnak, J. Juntaro, M. Sain, H. Manuspiya, Synthesis and Luminescence Properties of ZnS and Metal (Mn, Cu)-doped-ZnS Ceramic Powder, Solid state Sci. 14(2012) 299-304.
[24] L. Wang, H. Wei, Y. Fan, X. Liu, J. Zhan, Synthesis, Optical Properties, and Photocatalytic Activity of One-dimensional CdS@ZnS Core–shell Nano Composites, Nano Scale Res. Lett.4 (2009) 558-564